doi:10.1038/nature09820

Supplementary Figure 1, Tye et al.

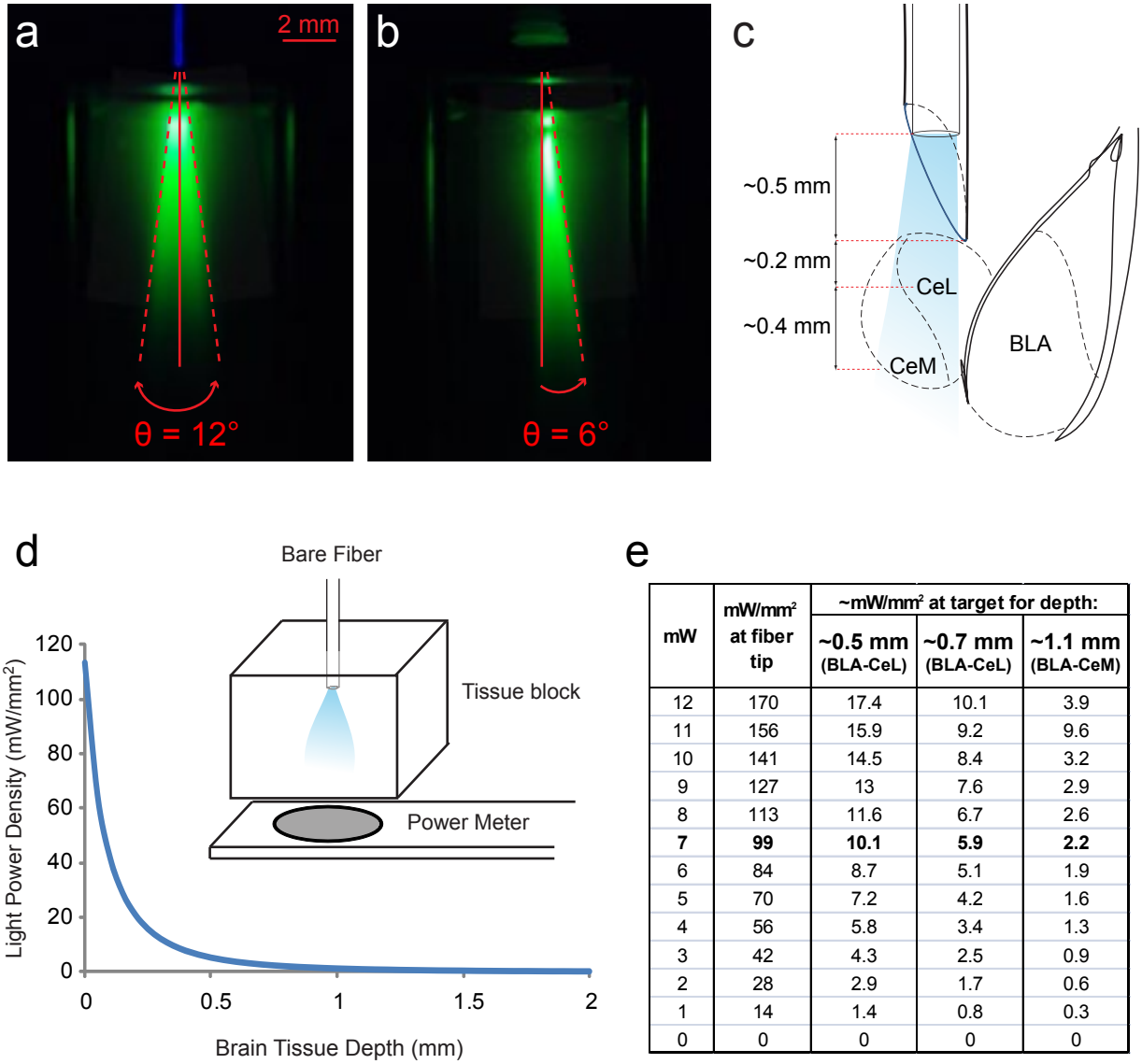

e

mW	mW/mm² at fiber tip	~mW/mm² at target for depth: ~0.5 mm (BLA-CeL)	~0.7 mm (BLA-CeL)	~1.1 mm (BLA-CeM)
12	170	17.4	10.1	3.9
11	156	15.9	9.2	9.6
10	141	14.5	8.4	3.2
9	127	13	7.6	2.9
8	113	11.6	6.7	2.6
7	**99**	**10.1**	**5.9**	**2.2**
6	84	8.7	5.1	1.9
5	70	7.2	4.2	1.6
4	56	5.8	3.4	1.3
3	42	4.3	2.5	0.9
2	28	2.9	1.7	0.6
1	14	1.4	0.8	0.3
0	0	0	0	0

Supplementary Figure 1: Beveled cannula and illumination profile design.

a) Light cone from bare fiber emitting 473 nm light over cuvette filled with fluorescein in water. The angle of the light cone is approximately 12 degrees. b) Light cone from the same fiber and light ensheathed in a beveled cannula. The beveled cannula blocks light delivery to one side, without detectably altering perpendicular light penetrance. c) Diagram of light delivery via the optical fiber with the beveled cannula over CeA. d) Chart indicating estimated light power density seen at various distances from the fiber tip in mouse brain tissue when the light power density seen at the fiber tip was 7 mW (~99 mW/mm^2). Inset, cartoon indicating the configuration. Optical fiber is perpendicular and aimed at the center of the power meter, through a block of mouse brain tissue. e) Table showing light power (mW) as measured by a standard power meter and the estimated light power density (mW/mm^2) seen at the tip, at the CeL (~0.5-0.7 mm depth in brain tissue) and at the CeM (~1.1 mm depth in brain tissue).

Supplementary Figure 2, Tye et al.

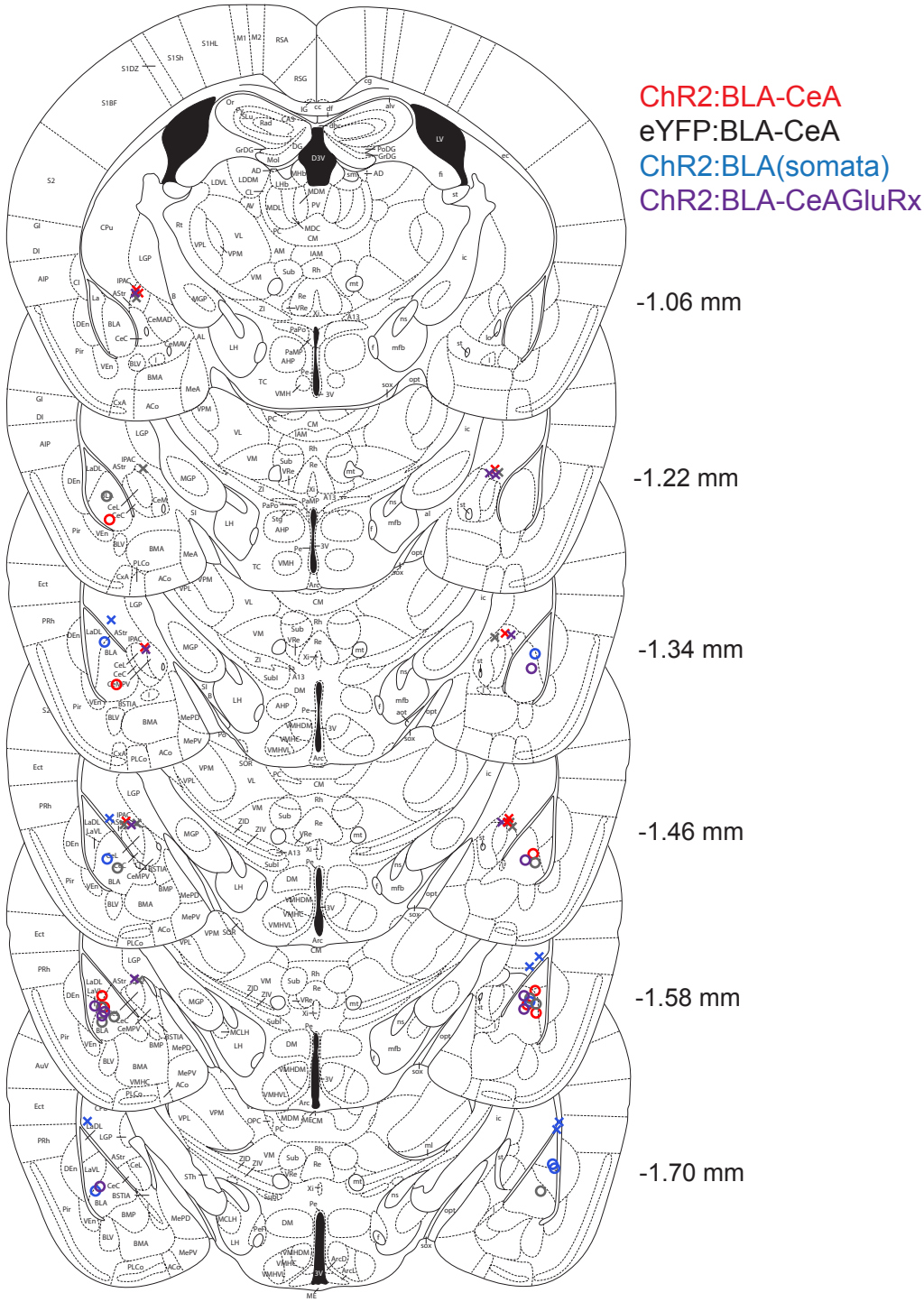

Supplementary Figure 2: Histologically verified placements of mice treated with 473 nm light.

Unilateral placements of the virus injection needle (circle) and the tip of beveled cannula (x) are indicated, counter-balanced for hemisphere. Colors indicate treatment group, see legend. Coronal sections containing the BLA and the CeA are shown here, numbers indicate the anteroposterior coordinates from bregma[1].

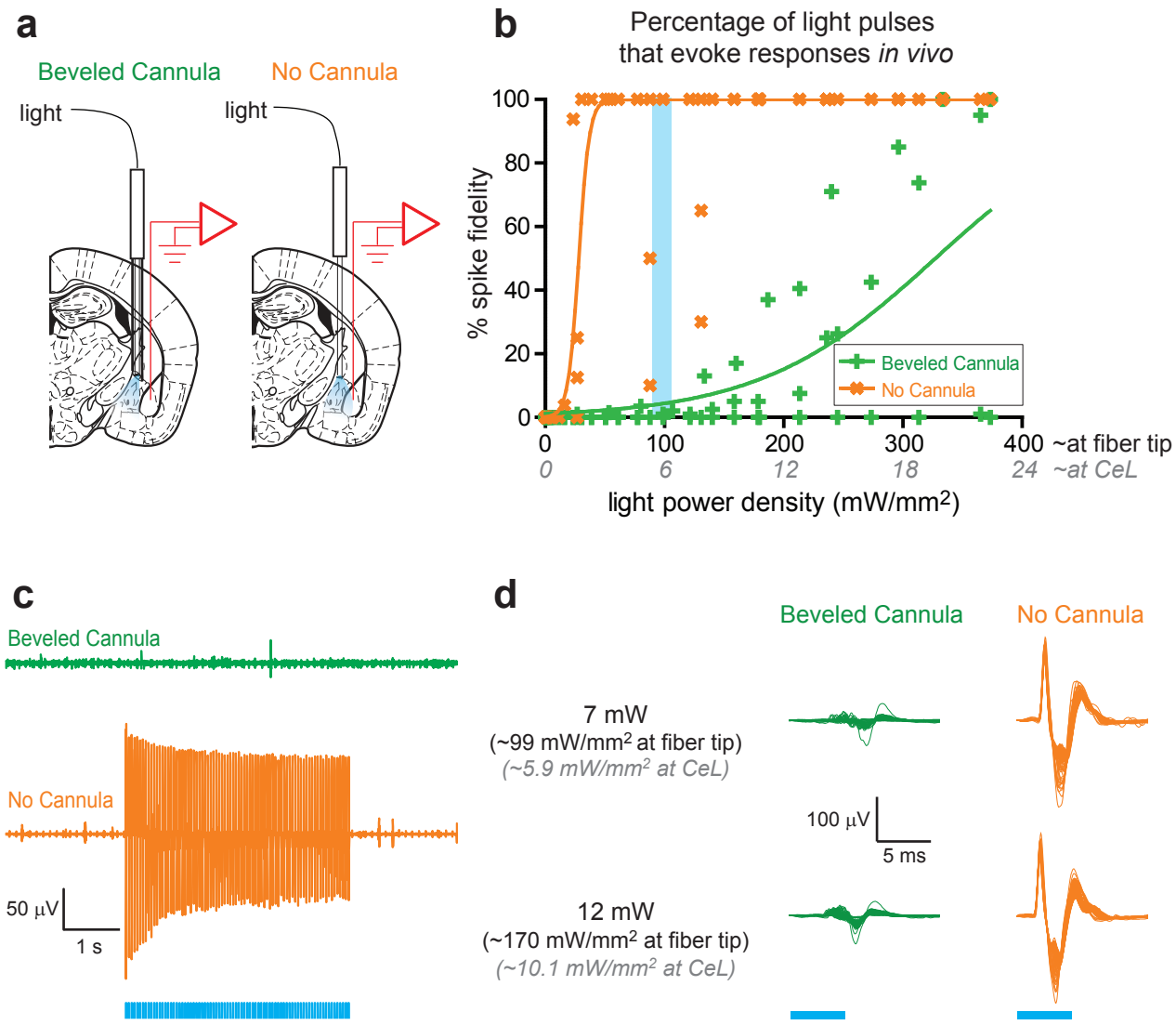

Supplementary Figure 3: Beveled cannula prevents light delivery to BLA and BLA spiking at light powers used for behavioral assays.

a) Schematic indicating the configuration of light delivery by optical fiber to the CeA and recording electrode (red) in the BLA. b) Scatterplot summary of recordings in the BLA with various light powers delivered to the CeA with and without the beveled cannula (n=4 sites). For each site, repeated alternations of recordings were made with and without the beveled cannula. The x-axis shows both the light power density at the fiber tip (black) and the estimated light power density at the CeL (grey). The blue shaded region indicates the range of light power densities used for behavioral assays (~7 mW; ~99 mW/mm^2 at the tip of the fiber). Reliable responses from BLA neurons were not observed in this light power density range. c) Representative traces of BLA recordings with 20 Hz 5ms pulse light stimulation at 7mW (~99 mW/mm^2 at fiber tip; ~5.9 mW/mm^2 at CeL) at the same recording site in the CeA. d) Population spike waveforms in response to single pulses of light reveal substantial light restriction even at high 12 mV power (~170 mW/mm^2 at the tip of the fiber; ~10.1 mW/mm^2 at CeL).

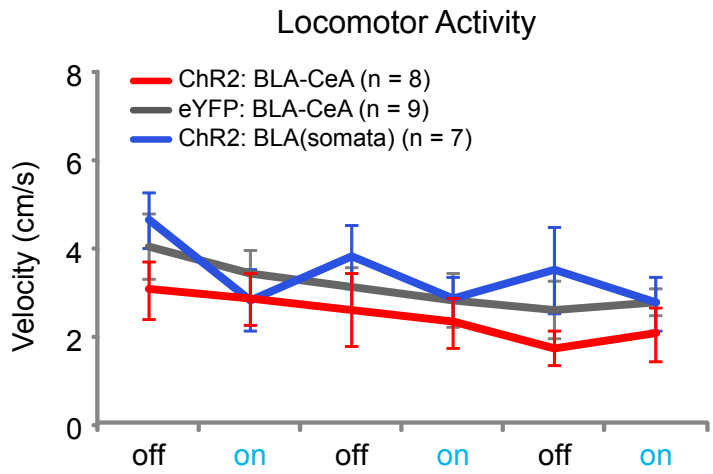

Supplementary Figure 4: Locomotor activity is not altered by unilateral photostimulation of BLA terminals in the CeA nor BLA somata.

Photostimulation did not significantly alter locomotor activity for any of the groups ($F_{5,108}$=1.4118; p=0.2257).

Supplementary Figure 5: Confocal images and c-fos quantification from the BLA, CeL and CeM from ChR2: BLA-CeA, eYFP:BLA-CeA and ChR2: BLA(somata) groups.

(a-b) Confocal image of a coronal section including CeA and BLA regions from a ChR2:BLA-CeA mouse (a) wherein 125μmx125μm squares indicate regions used for quantification, arranged in rows by group and in columns by region (b). **(c)** Percent of eYFP-positive and c-fos-positive neurons of DAPI-identified cells for all groups, by region. The ChR2:BLA (somata) group had a higher proportion of c-fos-positive BLA neurons relative to ChR2:BLA-CeA (**p<0.01) or eYFP:BLA-CeA (*p<0.05) groups. The ChR2:BLA-CeA group had a higher proportion of c-fos-positive cells in the CeL relative to the eYFP:BLA-CeA (*p<0.05), but not the ChR2:BLA (somata) group. Summary data for CeM neurons show no detectable differences among groups. White indicates DAPI, red indicates c-fos and green indicates YFP.

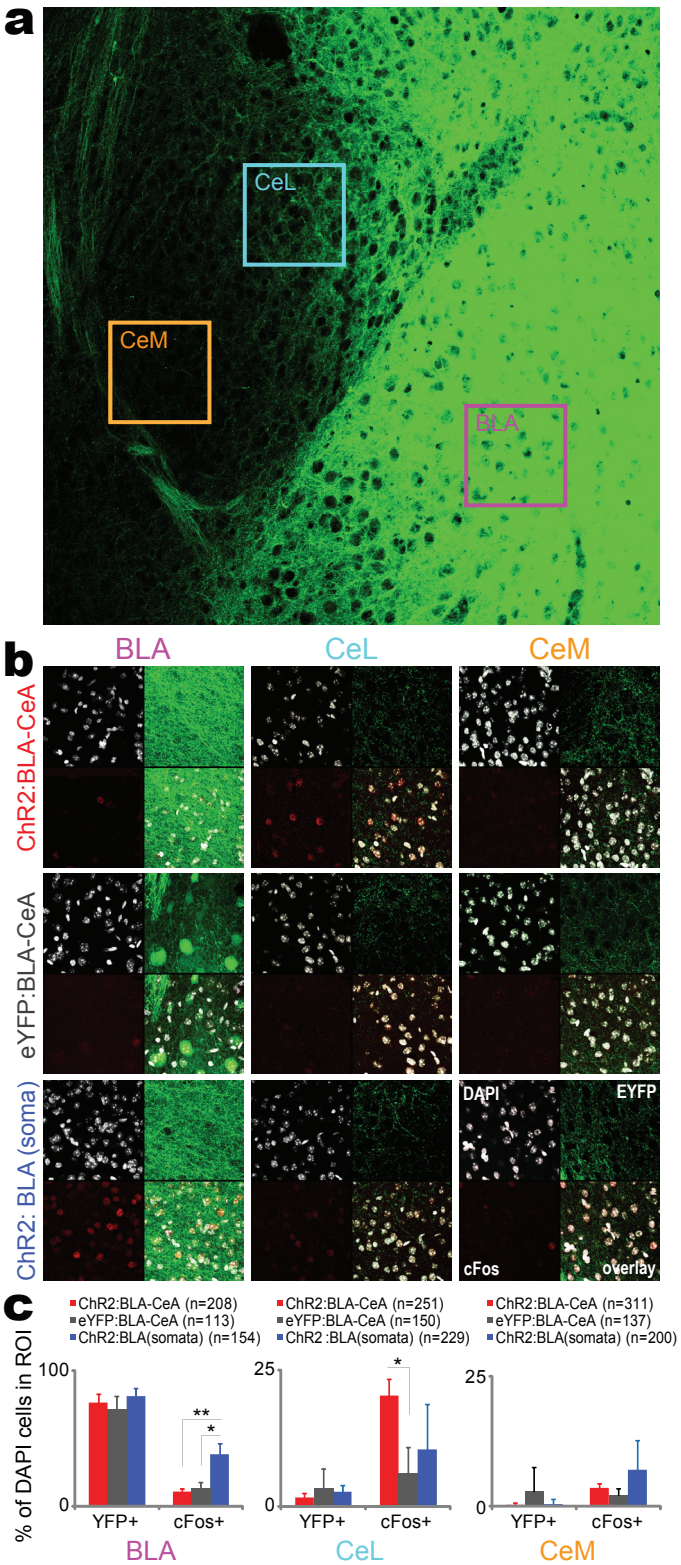

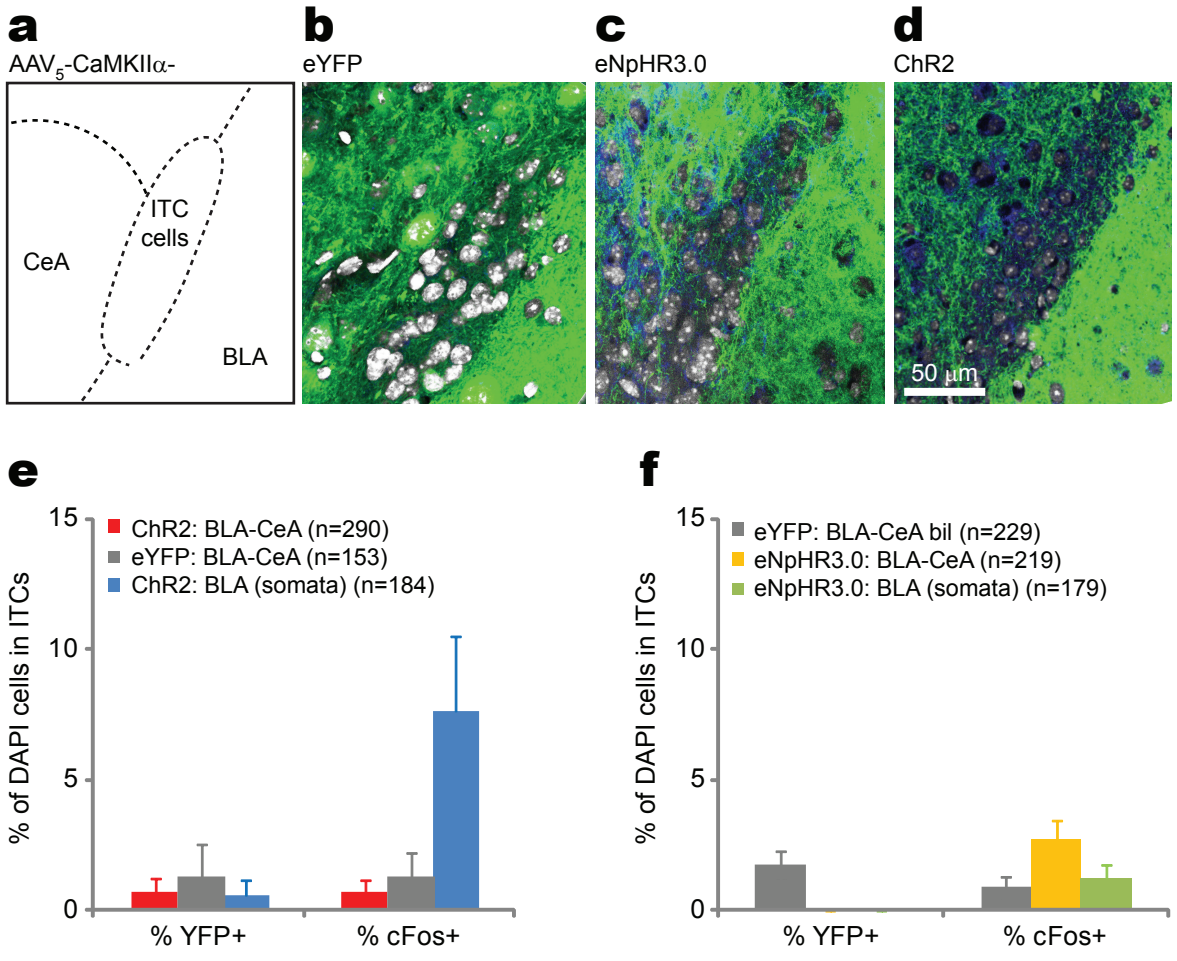

Supplementary Figure 6: Viral transduction excludes intercalated cell clusters.

a) Schematic of the intercalated cells displayed in subsequent confocal images. (b-d) Representative images of intercalated cells from mice that received eYFP (b), eNpHR3.0 (c) and ChR2 (d) injections into the BLA that were used for behavioral manipulations. Viral expression was not observed in intercalated cell clusters. (e-f) There were very low (<2%) levels of YFP expression in intercalated cell clusters for all 6 groups used in behavioral assays. There were no statistically significant differences among groups in c-fos expression.

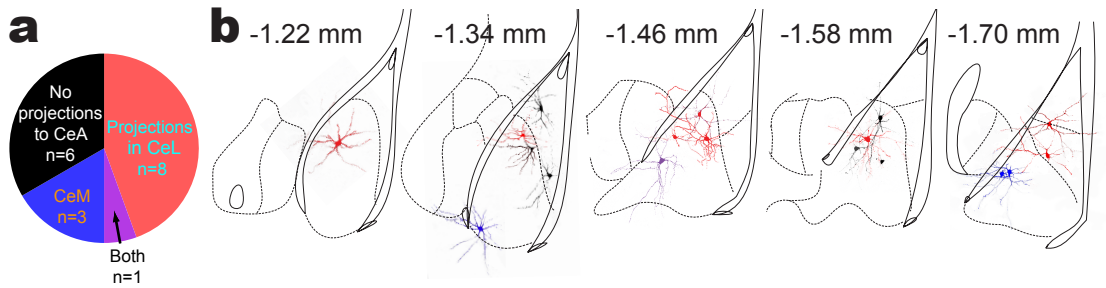

Supplementary Figure 7: Anatomical analysis of BLA neurons projecting to the CeL and CeM.

(a-b) 2-photon z-stack images of 18 dye-filled BLA neurons were reconstructed. Projections to the CeL and CeM are summarized in (a) and images shown in (b) wherein red, blue and purple indicate processes observed in CeL, CeM or both, respectively.

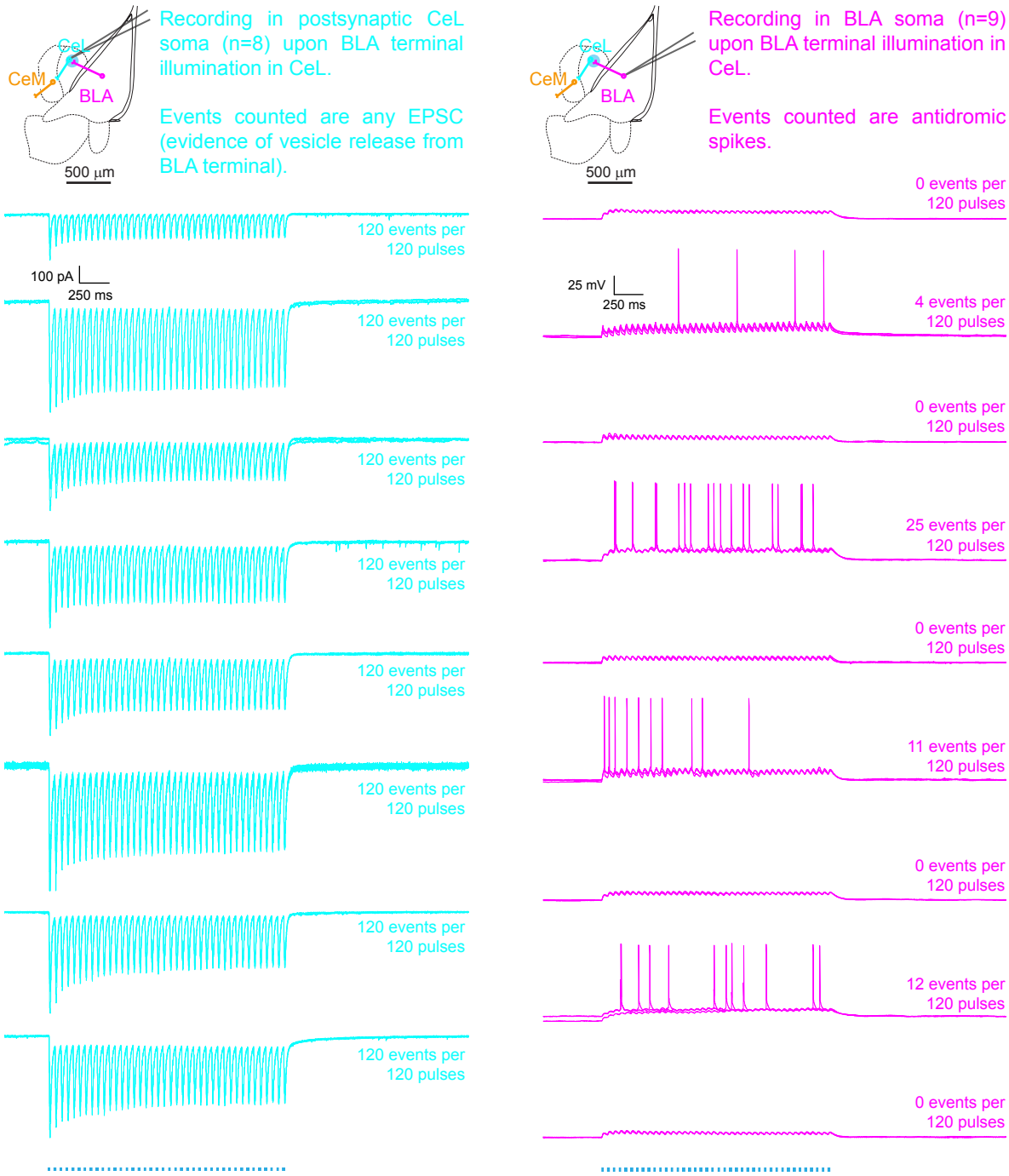

Supplementary Figure 8: Selective illumination of BLA terminals induces vesicle release onto CeL neurons without reliably eliciting antidromic action potentials.

Schematics and descriptions refer to the traces below, and trace color indicates cell type. Light illumination patterns are identical for both series of traces. Left column, CeL traces for three overlaid sweeps of a 40-pulse light train per cell (n=8). Here, time-locked EPSCs indicate vesicle release from the presynaptic ChR2-expressing BLA terminal, and for all postsynaptic CeL cells sampled, there were excitatory responses to 100% of light pulses. Right column, BLA traces for three overlaid 40-pulse sweeps per cell (n=9), with the mean number of light pulses delivered at the axon terminal resulting in a supra-threshold antidromic action potential (5.4%±2%, mean±SEM).

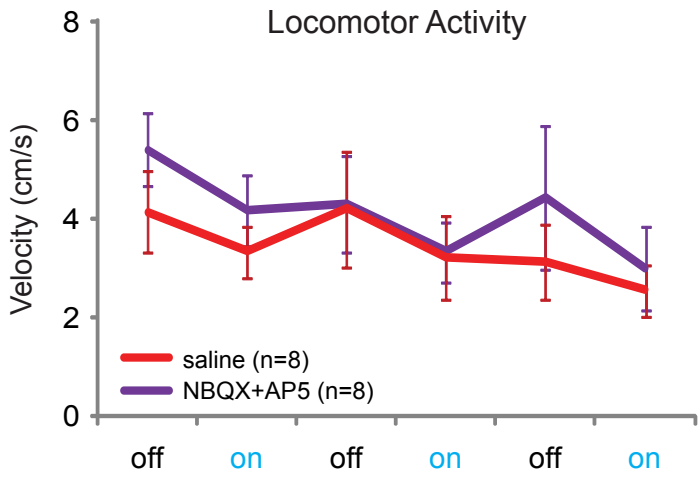

Supplementary Figure 9 Unilateral intra-CeA administration of glutamate antagonists does not alter locomotor activity.

Administration of NBQX and AP5 prior to the open field test did not impair locomotor activity (as measured by mean velocity) relative to saline infusion ($F_{1,77}$=2.34, p=0.1239).

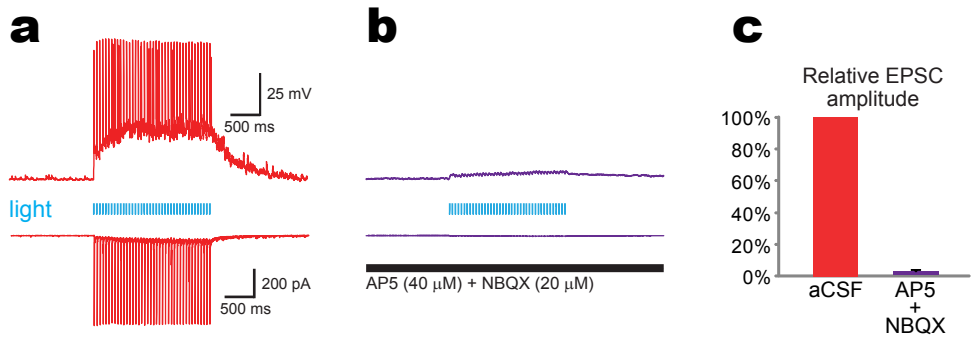

Supplementary Figure 10: Bath application of glutamate antagonists blocks optically-evoked synaptic transmission.

4-6 weeks following intra-BLA infusions of AAV_5-CamKII-ChR2-eYFP into the BLA of wild-type mice, we examined the ability of the glutamate receptor antagonists NBQX and AP5 to block glutamatergic transmission. a) Representative current-clamp (top) and voltage-clamp (bottom) traces of a representative CeL neuron upon a 20 Hz train of 473 nm light illumination of BLA terminals expressing ChR2. b) The same cell's responses following bath application of NBQX and AP5 show abolished spiking and EPSCs. c) Population summary (n=5) of the depolarizing current seen before and after bath application of NBQX and AP5, normalized to the pre-drug response.

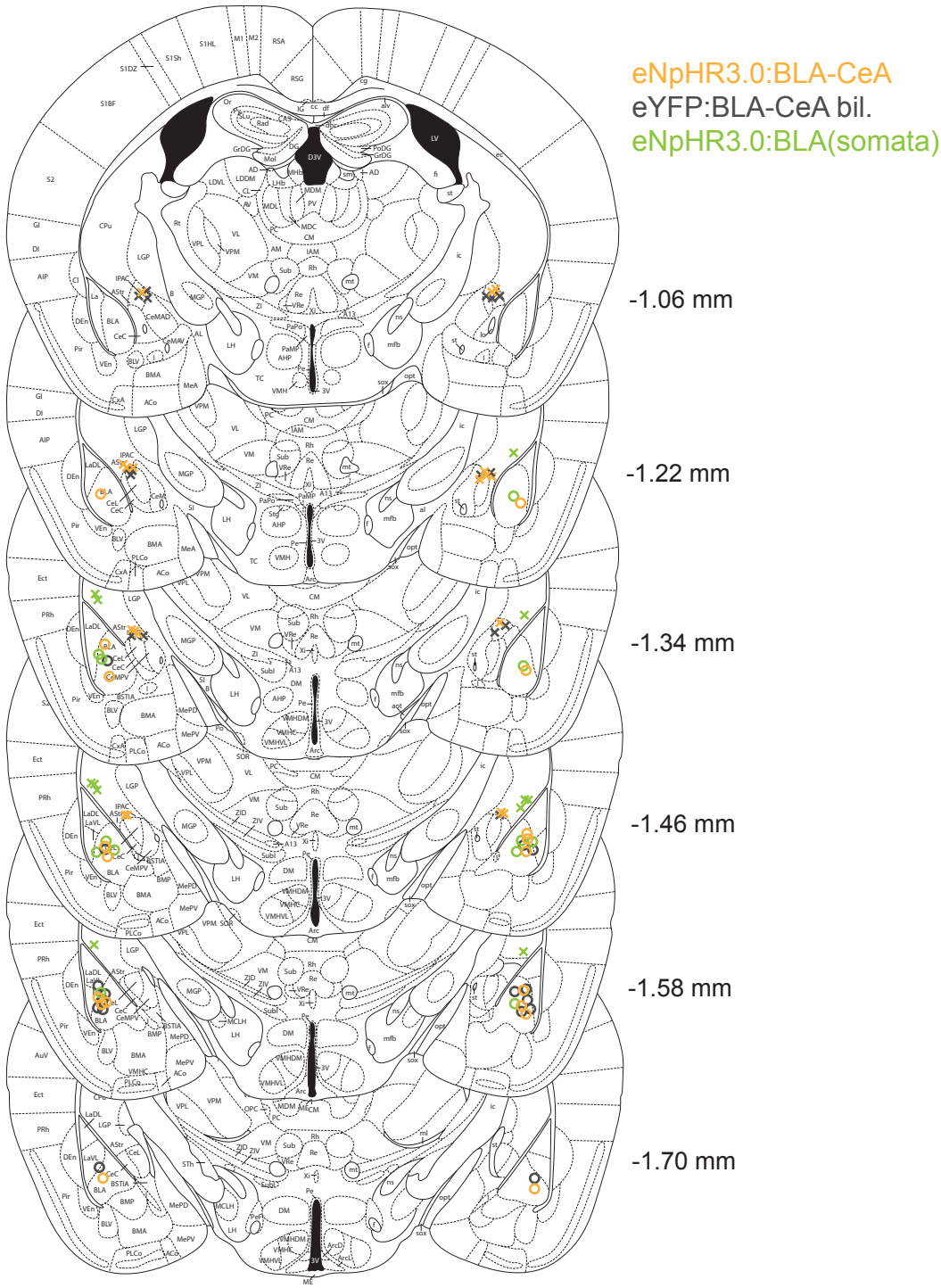

Supplementary Figure 11: Histologically verified placements of mice treated with 594 nm light.

Bilateral placements of virus injection needle (circle) and tip of beveled cannula (x) are indicated. Colors indicate treatment group, see legend. Coronal sections containing BLA and CeA are shown; numbers indicate AP coordinates from bregma[1].

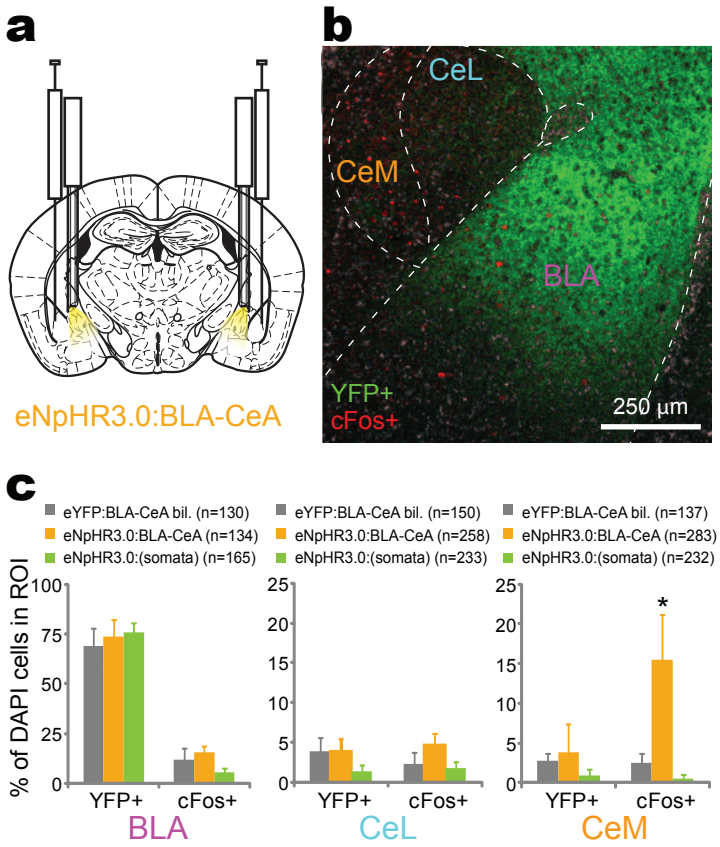

Supplementary Figure 12: Confocal images and c-fos quantification from the BLA, CeL and CeM from eNpHR3.0:BLA -CeA, eYFP:BLA-CeA and eNpHR3.0:BLA(somata) groups.

a) The eNpHR3.0:BLA-CeA group (n=9) received bilateral viral transduction of eNpHR3.0 in BLA neurons and cannula implantation to allow selective illumination of BLA terminals in the CeA. b) Confocal image of the BLA and CeA of a mouse treated with eNpHR3.0. (c-e) A higher proportion of CeM neurons (e) from the eNpHR3.0 group expressed c-fos relative to the eYFP group (*p<0.05).

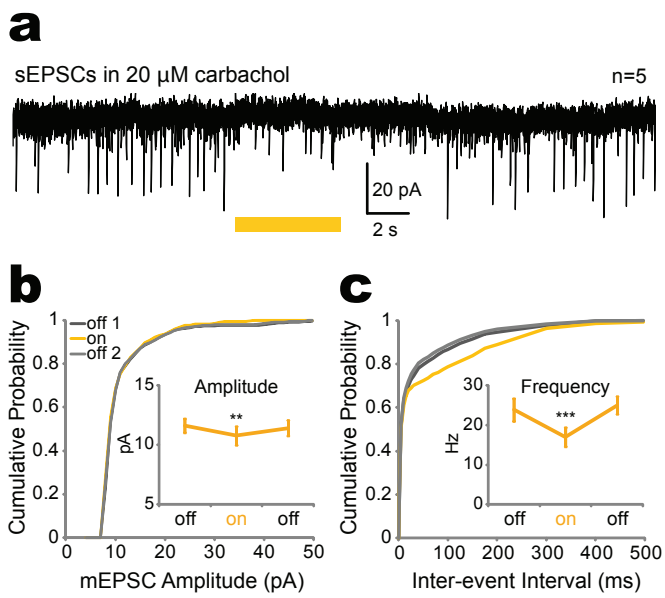

Supplementary Figure 13: Selective illumination of eNpHR3.0-expressing BLA terminals was sufficient to reduce spontaneous vesicle release.

(a-c) Representative CeL trace (a) show illumination of eNpHR3.0-expressing BLA terminals ~300µm away from the soma reduced sEPSC amplitude (b) and frequency (c) in the postsynaptic CeL neuron. Cumulative distribution histogram of sEPSC amplitude (b) and frequency (c) recorded from CeL neurons (n=5), insets show respective mean±SEM in epochs of matched duration before, during and after illumination (**p<0.01;***p<0.001).

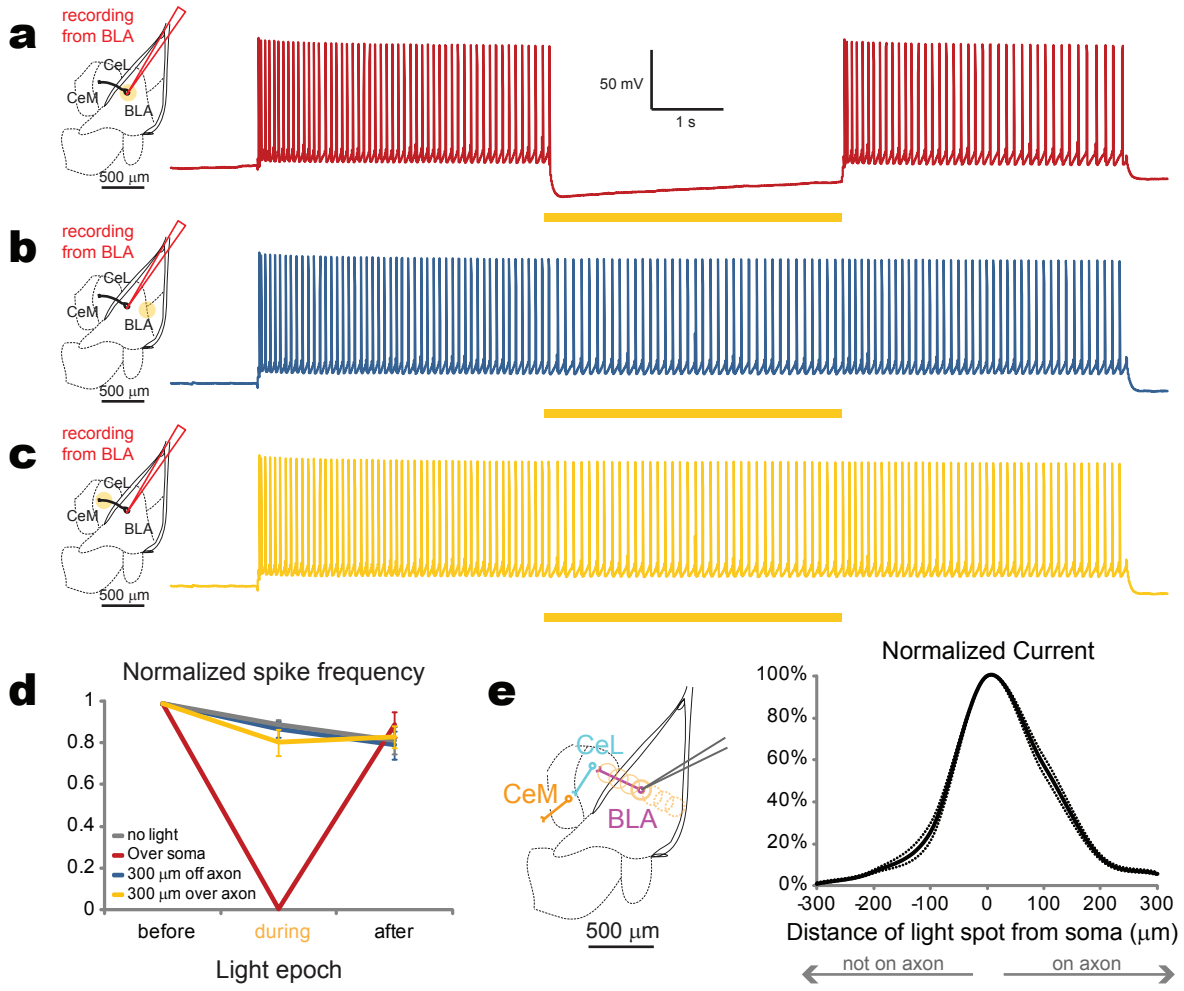

Supplementary Figure 14: Light stimulation parameters used in the eNpHR 3.0 terminal inhibition experiments does not block spiking at the cell soma.

(a-c) Schematics of the light spot location and recording sites alongside corresponding representative traces upon a current step lasting the duration of the spike train, paired with yellow light illumination at each location during the middle epoch (indicated by yellow bar). a) Representative current-clamp trace from a BLA neuron expressing eNpHR3.0 upon direct illumination shows potent inhibition of spiking during illumination of cell soma. b) Representative current-clamp trace from a BLA neuron expressing eNpHR3.0 when a ~125 µm diameter light spot is presented ~300 µm away from the cell soma without illuminating an axon. c) Representative current-clamp trace from a BLA neuron expressing eNpHR3.0 when a ~125 µm diameter light spot is presented ~300 µm away from the cell soma when illuminating an axon. d) While direct illumination of the cell soma induced complete inhibition of spiking that was significant from all other conditions ($F_{3,9}$=81.50, p<0.0001; n=3 or more per condition), there was no significant difference among the distal illumination ~300 µm away from the soma of BLA neurons expressing eNpHR3.0 conditions and the no light condition ($F_{2,7}$=0.79, p=0.49), indicating that distal illumination did not significantly inhibit spiking at the cell soma. e) Schematic indicating light spot locations relative to recording site, regarding the population summary shown to the right. Population summary shows the normalized hyperpolarizing current recorded from the cell soma per distance of light spot from cell soma, both on and off axon collaterals (n=5).

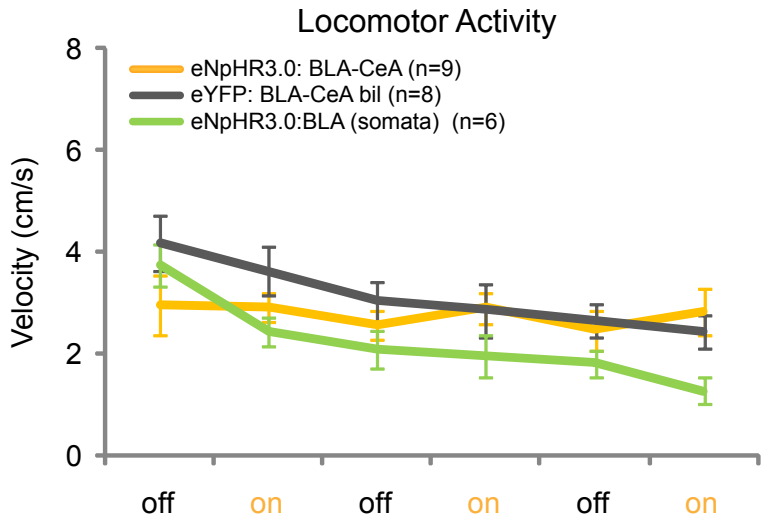

Supplementary Figure 15: Light stimulation does not alter locomotor activity in eNpHR3.0 and control groups.

There were no detectable differences in locomotor activity among groups nor light epochs ($F_{1,20}$=0.023, p=0.3892; $F_{1,100}$=3.08, p=0.086).

Materials and Methods

Subjects

Male C57BL/6 mice, aged 4-6 weeks at the start of experimental procedures, were maintained with a reverse 12-hr light/dark cycle and given food and water *ad libitum*. Animals shown in Figures 1, 2 and 3 (mice in the ChR2 Terminals, eYFP Terminals and ChR2 Cell Bodies groups) were all single-housed in a typical high-traffic mouse facility to increase baseline anxiety levels. Each mouse belonged to a single treatment group. Animals shown in Figure 4 (Bilateral eYFP and eNpHR3.0 groups) were group-housed in a special low-traffic facility to decrease baseline anxiety levels. Animal husbandry and all aspects of experimental manipulation of our animals were in accordance with the guidelines from the National Institute of Health and have been approved by members of the Stanford Institutional Animal Care and Use Committee.

Optical Intensity Measurements

Light transmission measurements were conducted with blocks of brain tissue from acutely sacrificed mice. The tissue was then placed over the photodetector of a power meter (Thorlabs, Newton, NJ) to measure the light power of the laser penetrated the tissue. The tip of a 300 μm diameter optical fiber was coupled to a 473 nm blue laser (OEM Laser Systems, East Lansing, MI). To characterize the light transmission to the opposite side of the bevel, the photodetector of the power meter was placed parallel to the beveled cannula. For visualization of the light cone, we used Fluorescein isothiocyanate-dextran (FD150s; Sigma, Saint Louis, MO) at approximately 5mg/ml placed in a cuvette with the optical fibers either with or without beveled cannula shielding aimed perpendicularly over the fluorescein solution. Power density at specific depths were calculated considering both fractional decrease in intensity due to the conical output of light from the optical fiber and the loss of light due to scattering in tissue (see Aravanis 2007, Gradinaru 2009). The half-angle of divergence θ_{div} for a multimode optical fiber, which determines the angular spread of the output light, is

$$\theta_{div} = \sin^{-1}\left(\frac{NA_{fib}}{n_{tis}}\right),$$

where n_{tis} is the index of refraction of gray matter (1.36, Vo-Dinh T 2003, Biomedical Photonics Handbook (Boca Raton, FL: CRC Press)) and NA_{fib} (0.37) is the numerical aperture of the optical fiber. The fractional change in intensity due to the conical spread of the light with distance (z) from the fiber end was calculated using trigonometry

$$\frac{I(z)}{I(z=0)} = \frac{\rho^2}{(z+\rho)^2}, where \ \rho = r\sqrt{\left(\frac{n}{NA}\right)^2 - 1}$$

and r is the radius of the optical fiber (100 μm).

The fractional transmission of light after loss due to scattering was modeled as a hyperbolic function using empirical measurements and the Kubelka-Munk model [1, 2], and the combined product of the power density at the tip of the fiber and the fractional changes due to the conical spread and light scattering, produces the value of the power density at a specific depth below the fiber.

Virus construction and packaging

The recombinant AAV vectors were serotyped with AAV_5 coat proteins and packaged by the viral vector core at the University of North Carolina. Viral titers were 2 x 10^{12} particles / mL, 3 x 10^{12} particles / mL, 4 x 10^{12} particles / mL respectively for AAV_5-CaMKIIα-hChR2(H134R)-eYFP, AAV_5-CaMKIIα-eYFP, and AAV_5-CaMKIIα-eNpHR3.0-eYFP. The pAAV-CaMKIIα-eNpHR3.0-eYFP plasmid was constructed by cloning CaMKIIα-eNpHR3.0-eYFP into an AAV backbone using MluI and EcoRI restriction sites. Similarly, The pAAV-CaMKIIα-eYFP plasmid was constructed by cloning CaMKIIα-eYFP into an AAV backbone using MluI and EcoRI restriction sites. The maps are available online at www.optogenetics.org.

Stereotactic injection and optical fiber placement

All surgeries were performed under aseptic conditions under stereotaxic guidance. Mice were anaesthetized using 1.5-3.0% isoflurane. All coordinates are relative to bregma in mm [3]. In all experiments, both *in vivo* and *in vitro*, virus was delivered to the BLA only, and any viral expression in the CeA rendered exclusion from all experiments. Cannula guides were beveled to form a 45-55 degree angle for the restriction of the illumination to the CeA. The short side of

the beveled cannula guide was placed antero-medially, the long side of the beveled cannula shielded the posterior-lateral portion of the light cone, facing the opposite direction of the viral injection needle. To preferentially target BLA-CeL synapses, we restricted opsin gene expression to BLA glutamatergic projection neurons and restricted light delivery to the CeA. Control of BLA glutamatergic projection neurons was achieved using an adeno-associated virus (AAV_5) vector carrying light-activated optogenetic control genes under the control of a CaMKIIα promoter. Within the BLA, CaMKIIα is only expressed in glutamatergic pyramidal neurons, not in local interneurons[4]. Mice in the ChR2 Terminals and eYFP Terminals groups received unilateral implantations of beveled cannulae for the optical fiber (counter-balanced for hemisphere), while mice in the eNpHR3.0 or respective eYFP group received bilateral implantations of the beveled cannulae over the CeA (-1.06 mm anteroposterior (AP); ±2.25 mm mediolateral (ML); and -4.4 mm dorsoventral (DV); PlasticsOne, Roanoke, VA)[3]. Mice in the ChR2 Cell Bodies groups received unilateral implantation of a Doric patchcord chronically implantable fiber (NA=0.22; Doric lenses, Quebec, Canada) over the BLA at (-1.6 mm AP; ±3.1 mm ML; -4.5 mm DV)[3]. For all mice, 0.5 µl of purified AAV_5 was injected unilaterally or bilaterally in the BLA (±3.1 mm AP, 1.6 mm ML, -4.9 mm DV)[3] using beveled 33 or 35 gauge metal needle facing postero-lateral side to restrict the viral infusion to the BLA. 10 µl Hamilton microsyringe (nanofil; WPI, Sarasota, FL) were used to deliver concentrated AAV solution using a microsyringe pump (UMP3; WPI, Sarasota, FL) and its controller (Micro4; WPI, Sarasota, FL). Then, 0.5 µl of virus solution was injected at each site at a rate of 0.1 µl per min. After injection completion, the needle was lifted 0.1 mm and stayed for 10 additional minutes and then slowly withdrawn. One layer of adhesive cement (C&B metabond; Parkell, Edgewood, NY) followed by cranioplastic cement (Dental cement; Stoelting, Wood Dale, IL) was used to secure the fiber guide system to the skull. After 20 min, the incision was closed using tissue adhesive (Vetbond; Fisher, Pittsburgh, PA). The animal was kept on a heating pad until it recovered from anesthesia. A dummy cap (rat: C312G, mouse: C313G) was inserted to keep the cannula guide patent. Behavioral and electrophysiological experiments were conducted 4-6 weeks later to allow for viral expression.

In vivo recordings

Simultaneous optical stimulation of central amygdala (CeA) and electrical recording of basolateral amygdala (BLA) of adult male mice previously (4-6 weeks prior) transduced in BLA with AAV-CaMKIIα-ChR2-eYFP viral construct was carried out as described previously[2]. Animals were deeply anesthetized with isoflurane prior to craniotomy and had negative toe pinch. After aligning mouse stereotaxically and surgically removing approximately 3mm^2 skull dorsal to amygdala. Coordinates were adjusted to allow for developmental growth of the skull and brain, as mice received surgery when they were 4-6 weeks old and experiments were performed when the mice were 8-10 weeks old (centered at -1.5mm AP, ±2.75mm ML)[3], a 1Mohm 0.005-in extracellular tungsten electrode (A-M systems) was stereotactically inserted into the craniotomized brain region above the BLA (in mm: -1.65 AP, ±3.35 ML, -4.9 DV)[3]. Separately, a 0.2 N.A. 200 μm core diameter fiber optic cable (Thorlabs) was stereotactically inserted into the brain dorsal to CeA (-1.1 AP, ±2.25 ML, -4.2 DV)[3]. After acquiring a light evoked response, voltage ramps were used to vary light intensity during stimulation epochs (20 Hz, 5 ms pulse width) 2s in length. After acquiring optically evoked signal, the exact position of the fiber was recorded, the fiber removed from the brain, inserted into a custom beveled cannula, reinserted to the same position, and the same protocol was repeated. In most trials, the fiber/cannula was then extracted from the brain, the cannula removed, and the bare fiber reinserted to ensure the fidelity of the population of neurons emitting the evoked signal. Recorded signals were bandpass filtered between 300 Hz and 20 kHz, AC amplified either 1000x or 10000x (A-M Systems 1800), and digitized (Molecular Devices Digidata 1322A) before being recorded using Clampex software (Molecular Devices). Clampex software was used for both recording field signals and controlling a 473nm (OEM Laser Systems) solidstate laser diode source coupled to the optrode. Light power was titrated between < 1 mW (~14 mW/mm^2) and 28 mW (~396 mW/mm^2) from the fiber tip and measured using a standard light power meter (Thorlabs). Electrophysiological recordings were initiated approximately 1mm dorsal to BLA after lowering isoflurane anesthesia to a constant level of 1%. Optrode was lowered ventrally in ~0.1mm steps until localization of optically evoked signal.

Behavioral assays

All animals used for behavior received viral transduction of BLA neurons and the implantation enabling unilateral (for ChR2 groups and controls) or bilateral (for eNpHR3.0 groups and

controls) light delivery. For behavior, multimode optical fibers (NA 0.37; 300 μm core, BFL37-300; Thorlabs, Newton, NJ) were precisely cut to the optimal length for restricting the light to the CeA, which was shorter than the long edge of the beveled cannula, but longer than the shortest edge of the beveled cannula. For optical stimulation, the fiber was connected to a 473 nm or 594 nm laser diode (OEM Laser Systems, East Lansing, MI) through an FC/PC adapter. Laser output was controlled using a Master-8 pulse stimulator (A.M.P.I., Jerusalem, Israel) to deliver light trains at 20 Hz, 5 ms pulse-width for 473 nm light, and constant light for 594 nm light experiments. All included animals had the center of the viral injection located in the BLA, though there was sometimes leak to neighboring regions or along the needle tract. Any case in which there was any detectable viral expression in the CeA, the animals were excluded. All statistically significant effects of light were discussed, and undiscussed comparisons did not show detectable differences.

The elevated plus maze was made of plastic and consisted of two light gray open arms (30 × 5 cm), two black enclosed arms (30 × 5 × 30 cm) extending from a central platform (5 × 5 × 5 cm) at 90 degrees in the form of a plus. The maze was placed 30 cm above the floor. Mice were individually placed in the center. 1-5 minutes were allowed for recovery from handling before the session was initiated. Video tracking software (BiObserve, Fort Lee, NJ) was used to track mouse location, velocity and movement of head, body and tail. All measurements displayed were relative to the mouse body. Light stimulation protocols are specified by group. ChR2:BLA-CeA mice and corresponding controls groups (eYFP:BLA-CeA and ChR2:BLA Somata) were singly-housed in a high-stress environment for at least 1 week prior to anxiety assays: unilateral illumination of BLA terminals in the CeA at 7-8 mW (~106 mW/mm^2 at the tip of the fiber, ~6.3 mW/mm^2 at CeL and ~2.4 mW/mm^2 at the CeM) of 473 nm light pulse trains (5 ms pulses at 20 Hz). For the ChR2 Cell Bodies group BLA neurons were directly illuminated with a lower light power because illumination with 7-8 mW induced seizure activity, so we unilaterally illuminated BLA neurons at 3-5 mW (~57 mW/mm^2) of 473 nm light pulse trains (5 ms pulses at 20 Hz). For the eNpHR3.0 and corresponding eYFP group, all mice were group-housed and received bilateral viral injections and bilateral illumination of BLA terminals in the CeA at 4-6 mW (~71 mW/mm^2 at the tip of the fiber, ~4.7 mW/mm^2 at the CeL and ~1.9 mW/mm^2 at the CeM) of 594 nm light with constant illumination throughout the 5-min light on epoch. The 15-min session was divided into 3 5-min epochs, the first epoch there was no light stimulation (off), the second epoch light was delivered as specified above (on), and the third epoch there was no light stimulation (off).

The open-field chamber (50 × 50 cm) and the open field was divided into a central field (center, 23 × 23 cm) and an outer field (periphery). Individual mice were placed in the periphery of the field and the paths of the animals were recorded by a video camera. The total distance traveled was analyzed by using the same video-tracking software, Viewer^2 (BiObserve, Fort Lee, NJ). The open field assessment was made immediately after the elevated-plus maze test. The open field test consisted of an 18-min session in which there were six 3-min epochs. The epochs alternated between no light and light stimulation periods, beginning with a light off epoch. For all analyses and charts where only "off" and "on" conditions are displayed, the 3 "off" epochs were pooled and the 3 "on" epochs were pooled.

For the glutamate receptor antagonist manipulation, a glutamate antagonist solution consisting of 22.0 mM of NBQX and 38.0 mM of D-APV (Tocris, Ellisville, MO) dissolved in saline (0.9% NaCl). 5-15 min before the anxiety assays, 0.3 µl of the glutamate antagonist solution was infused into the CeA via an internal infusion needle, inserted into the same guide cannulae used for light delivery via optical fiber, that was connected to a 10-µl Hamilton syringe (nanofil; WPI, Sarasota, FL). The flow rate (0.1 µl per min) was regulated by a syringe pump (Harvard Apparatus, MA). Placements of the viral injection, guide cannula and chronically-implanted fiber were histologically verified as indicated in Supplementary Figs 1 and 4.

Two-photon optogenetic circuit mapping and *ex vivo* electrophysiological recording

Mice were injected with AAV_5-CaMKIIα-ChR2-eYFP at 4 weeks of age, and were sacrificed for acute slice preparation 4-6 weeks to allow for viral expression. Coronal slices containing the BLA and CeA were prepared to examine the functional connectivity between the BLA and the CeA. Two-photon images and electrophysiological recordings were made under the constant perfusion of aCSF, which contained (in mM): 126 NaCl, 26 NaHCO3, 2.5 KCl, 1.25 NaH2PO4, 1 MgCl2, 2 CaCl, and 10 glucose. All recordings were at 32°C. Patch electrodes (4-6 MOhms) were filled (in mM): 10 HEPES, 4 Mg-ATP, 0.5 MgCl2, 0.4 Na3-GTP, 10 NaCl, 140 potassium gluconate, and 80 Alexa-Fluor 594 hydrazide (Molecular Probes, Eugene OR). Whole-cell patch-clamp recordings were performed in BLA, CeL and CeM neurons, and cells were allowed to fill for approximately 30 minutes before imaging on a modified two-photon microscope (Prairie Microscopes, Makison WI) where two-photon imaging, whole-cell recording and optogenetic stimulation could be done simultaneously. Series resistance of the pipettes was usually 10–20 MOhms. Blue light pulses were elicited using a 473nm LED at ~7mW/mm^2 (Thorlabs, Newton

NJ) unless otherwise noted. A Coherent Ti-Saphire laser was used to image both ChR2-YFP (940 nm) and Alexa-Fluor 594 (800 nm). A FF560 dichroic with filters 630/69 and 542/27 (Semrock, Rochester NY) was also used to separate both molecules' emission. All images were taken using a 40X/.8 NA LUMPlanFL/IR Objective (Olympus, Center Valley PA). In order to isolate fibers projecting to CeL from the BLA and examine responses in the CeM, slices were prepared as described above with the BLA excluded from illumination. Whole-cell recordings were performed in the CeM with illumination from the objective aimed over the CeL. To further ensure activation of terminals from the BLA to CeL was selective, illumination was restricted to a ~125 μm diameter around the center of the CeL. Here, blue light pulses were elicited using an XCite halogen light source (EXPO, Mississauga, Ontario) with a 470/3 filter at 6.5 mW/mm2 coupled to a shutter (Uniblitz, Rochester NY). For functional mapping, we first recorded from a BLA neuron expressing ChR2 and simultaneously collected electrophysiological recordings and filled the cell with Alexa-Fluor 594 hydrazide dye to allow for two-photon imaging. Two-photon z-stacks were collected at multiple locations along the axon of the filled BLA neuron. We then followed the axon of the BLA neuron projecting to the CeL nucleus and recorded from a CeL neuron in the BLA terminal field. We then simultaneously recorded from a CeL neuron, filled the cell with dye and performed two-photon live imaging before following the CeL neuronal axons to the CeM. We then repeated this procedure in a CeM neuron, but moved the light back to the terminal field in the CeL to mimic the preferential illumination of BLA-CeL synapses with the same stimulation parameters as performed *in vivo*. Voltage-clamp recordings were made at both -70 mV, to isolate EPSCs, and at 0 mV, to isolate IPSCs. EPSCs were confirmed to be EPSCs via bath application of the glutamate receptor antagonists (n = 5), NBQX (22 μM) and AP5 (38 μM), IPSCs were confirmed to be IPSCs via bath application of bicuculline (10 μM; n = 2), which abolished them, respectively. We also performed current-clamp recordings when the cell was resting at approximately -70 mV.

For the characterization of optogenetically-driven antidromic stimulation in BLA axon terminals, animals were injected with AAV_5-CaMKIIα-ChR2-eYFP at 4 weeks of age, and were sacrificed for acute slice preparation 4-6 weeks to allow for viral expression. Slice preparation was the same as above. To the aCSF we added 0.1 mM picrotoxin, 10 μM CNQX and 25 μM AP5 (Sigma, St. Louis, MO). Whole-cell patch-clamp recordings were performed in BLA neurons and were allowed to fill for approximately 30 minutes before two-photon imaging. Series resistance of the pipettes was usually 10–20 MOhms. All images were taken using a 40X/.8 NA LUMPlanFL/IR Objective (Olympus, Center Valley PA). Blue light pulses were elicited using an

XCite halogen light source (EXPO, Mississauga, Ontario) with a 470/30 filter at 6.5 mW/mm^2 coupled to a shutter (Uniblitz, Rochester NY). Two-photon z-stacks were collected at multiple locations along the axon of the filled BLA neuron. Only neurons whose axons could be visualized for over ~300 μm diameter towards the CeL nucleus were included for the experiment, and neurons that had processes going in all directions were also excluded. Stimulation on/off axon was accomplished by moving the slice relative to a ~125 μm diameter blue light spot. In order to calibrate the slice for correct expression, whole-cell patch-clamp was performed on a CeL cell and a ~125 μm diameter spot blue pulse was used to ensure that synaptic release from the BLA terminals on to the CeL neuron was reliable.

For the dissection of direct and indirect projections to CeM, animals were injected with AAV_5-CaMKIIα-ChR2-eYFP at 4 weeks of age, and were sacrificed for acute slice preparation 4-6 weeks to allow for viral expression. Slice preparation was the same as above. Light was delivered through a 40X/.8 NA LUMPlanFL/IR Objective (Olympus, Center Valley PA). Prior to whole cell patch clamping in the CeM nucleus, the location of the CeL nucleus was noted in order to revisit it with the light spot restricted to this region. Whole-cell patch-clamp recordings were performed in CeM neurons. Series resistance of the pipettes was usually 10–20 MOhms. Blue light pulses were elicited using a XCite halogen light source (EXPO, Mississauga, Ontario) with a 470/30 filter at 6.5 mW/mm^2 coupled to a shutter (Uniblitz, Rochester NY). During CeM recordings, broad illumination (~425-450 μm in diameter) of BLA terminals in the CeA and 20 Hz, 5 ms light train for 2s was applied. Voltage-clamp recordings were made at 70mV and 0mV to isolate EPSCs and IPSCs respectively. Current-clamp recordings were also made. Then, illumination was moved to the CeL using a restricted light spot ~125 μm in diameter. We again performed voltage clamp recordings at -70mV and 0mV and used 20 Hz, 5 ms light train for 2s. For the CeM neuron spiking inhibition experiments, in current-clamp, we applied the minimal current step required to induce spiking (~60pA) and simultaneously applied preferential illumination of ChR2-expressing BLA terminals in the CeL with a 20 Hz, 5 ms light train for 2s (mean over 6 sweeps per cell). For the experiments comparing the broad illumination of the BLA terminal field centered in the CeM to selective illumination of BLA-CeL terminals, these conditions were performed in repeated alternation in the same CeM cells (n=7).

To verify that terminal inhibition did not alter somatic spiking, animals were injected with AAV_5-CaMKIIα-eNpHR3.0-eYFP at 4 weeks of age, and were sacrificed for acute slice preparation 4-6 weeks to allow for viral expression. Slice preparation was the same as above. Whole-cell patch-clamp recordings were performed in BLA neurons and were allowed to fill for

approximately 30 minutes. Light was delivered through a 40X/.8 NA LUMPlanFL/IR Objective (Olympus, Center Valley PA). Whole-cell patch-clamp recordings were performed on BLA neurons. Series resistance of the pipettes was usually 10–20 MOhms. Yellow light pulses were elicited using a XCite halogen light source (EXPO, Mississauga, Ontario) with a 589/24 filter at 6.5 mW/mm^2 coupled to a shutter (Uniblitz, Rochester NY). After patching, an unrestricted light spot (~425-450 microns in diameter) was placed over the BLA soma and a 1s pulse was applied. Cells were excluded if the current recorded was under 600 pA of hyperpolarizing current and the axon did not travel over ~300 μm towards the CeL nucleus. The light spot was then restricted to ~125 μm in diameter. On and off axon voltage clamp recordings were taken with a 1s pulse of light. For the current clamp recordings, action potentials were generated by applying 250 pA of current to the cell soma through the patch pipette.

To demonstrate that selective illumination of eNpHR3.0-expressing BLA terminals reduced the probability of spontaneous vesicle release, animals were injected with AAV$_5$-CaMKIIα-eNpHR3.0-eYFP at 4 weeks of age, and were sacrificed for acute slice preparation 4-6 weeks to allow for viral expression. Slice preparation was the same as above. Whole-cell patch-clamp recordings were performed in central lateral neurons. Light was delivered through a 40X/.8 NA LUMPlanFL/IR Objective (Olympus, Center Valley PA). Series resistance of the pipettes was usually 10–20 MOhms. Yellow light pulses were elicited using a XCite halogen light source (EXPO, Mississauga, Ontario) with a 589/24 filter at 6.5 mW/mm^2 coupled to a shutter (Uniblitz, Rochester NY). The light spot was restricted to ~125 μm in diameter. Carbachol was added to the bath at a concentration of 20 μM. After sEPSC activity increased in the CeL neuron, light pulses were applied ranging in times from 5s to 30s.

To demonstrate that selective illumination of eNpHR3.0-expressing BLA terminals could reduce the probability of vesicle release evoked by electrical stimulation, animals were injected with AAV$_5$-CaMKIIα-eNpHR3.0-eYFP at 4 weeks of age, and were sacrificed for acute slice preparation 4-6 weeks to allow for viral expression. Slice preparation was the same as above. A bipolar concentric stimulation probe (FHC, Bowdoin ME) was placed in the BLA. Whole-cell patch-clamp recordings were performed in CeL neurons. Light was delivered through a 40X/.8 NA LUMPlanFL/IR Objective (Olympus, Center Valley PA). Series resistance of the pipettes was usually 10–20 MOhms. Amber light pulses over the central lateral cell were elicited using a XCite halogen light source (EXPO, Mississauga, Ontario) with a 589/24 filter at 6.5 mW/mm^2 coupled to a shutter (Uniblitz, Rochester NY). The light spot was restricted to ~125 μm in

diameter. Electrical pulses were delivered for 40 seconds and light was delivered starting at 10 seconds and shut off at 30 seconds in the middle.

For the anatomical tracing experiments, neurons were excluded when the traced axons were observed to be severed and all BLA neurons included in the anatomical assay (Fig. 3a,b) showed spiking patterns typical of BLA pyramidal neurons[18] upon a current step.

Slice immunohistochemistry

Anesthetized mice were transcardially perfused with ice-cold 4% paraformaldehyde (PFA) in PBS (pH 7.4) 100-110 min after termination of *in vivo* light stimulation. Brains were fixed overnight in 4% PFA and then equilibrated in 30% sucrose in PBS. 40 µm-thick coronal sections were cut on a freezing microtome and stored in cryoprotectant at 4ºC until processed for immunohistochemistry. Free-floating sections were washed in PBS and then incubated for 30 min in 0.3% Tx100 and 3% normal donkey serum (NDS). Primary antibody incubations were performed overnight at 4 °C in 3% NDS/PBS (rabbit anti-c-fos 1:500, Calbiochem, La Jolla, CA; mouse anti-CaMKII 1:500, Abcam, Cambridge, MA). Sections were then washed and incubated with secondary antibodies (1:1000) conjugated to Cy3 or Cy5 (Jackson Laboratories, West Grove, PA) for 3 hrs at room temperature. Following a 20 min incubation with DAPI (1:50,000) sections were washed and mounted on microscope slides with PVD-DABCO.

Confocal microscopy and analysis

Confocal fluorescence images were acquired on a Leica TCS SP5 scanning laser microscope using a 20X/0.70NA or a 40X/1.25NA oil immersion objective. Serial stack images covering a depth of 10 µm through multiple sections were acquired using equivalent settings. The Volocity image analysis software (Improvision / PerkinElmer, Waltham, MA) calculated the number of c-fos positive cells per field by thresholding c-fos immunoreactivity above background levels and using the DAPI staining to delineate nuclei. All imaging and analysis was performed blind to the experimental conditions.

Statistics

For behavioral experiments and the *ex vivo* electrophysiology data, binary comparisons were tested using nonparametric bootstrapped t-tests (paired or unpaired where appropriate)[5], while hypotheses involving more than two group means were tested using linear contrasts (using the "boot" and "lme4" packages in R[6], respectively); the latter were formulated as contrasts between coefficients of a linear mixed-effects model (a "two-way repeated-measures ANOVA") with the fixed effects being the genetic or pharmacological manipulation and the light treatment (on or off). All hypothesis tests were specified *a priori*. Subjects were modeled as a random effects. For c-fos quantification comparisons, we used a one-way ANOVA followed by Tukey's multiple comparisons test.

Plots of the data clearly show a relationship between observation mean and observation variance (that is, they are heteroskedastic; see for example, Figure 1e and Figure 3j). We found that a standard square-root transformation corrected this well. Additionally, eNpHR3.0 elevated plus maze (EPM) data required detrending by a linear fit over time to account for a decrease in exploration behavior over time. As is standard for a two-way linear mixed effects model (also known as a two-way repeated-measures ANOVA), we model (the square-root corrected value of) the kth observation in the ijth cell (y_{ijk}) as

$$\sqrt{y_{ijk}} = \mu + c_i + t_j + (c:t)_{ij} + b_j + e_{ijk} \quad (1)$$

where

- μ is the grand mean across all cells (where the ijth "cell" in the collection of observations corresponding to the ith condition and jth treatment)
- c_i is a fixed effect due to the ith animal condition across treatments (for example, a genetic manipulation)
- t_j is a fixed effect due to the jth treatment across conditions (for example, light on or light off)
- $(c:t)_{ij}$ is a fixed effect due to the interaction of the ith condition and jth treatment in the ijth cell
- b_j is a random effect corresponding to animals being used across treatments, and
- e_{ijk} is an independent and identically distributed (i.i.d.) random normal disturbance in the ijkth observation with mean 0 and variance σ^2, and independent of b_j for all j

Collecting the fixed effects into a 2-way analysis of variance (ANOVA) design matrix $X \in \mathbb{R}^{n \times p}$, dummy coding the random effects in a sparse matrix $Z \in \mathbb{R}^{n \times q}$, and letting $\tilde{y} = \sqrt{y}$ we can express the model in matrix form as

$$\tilde{y} = X\beta + Zb + e \tag{2}$$

where $\tilde{y} \in \mathbb{R}^n$, $b \in \mathbb{R}^q$, and $e \in \mathbb{R}^n$ are observations of random variables $\tilde{\mathcal{Y}}$, $\mathcal{B}$, and ϵ respectively and our model assumes

$$\begin{aligned} \mathcal{B} &\sim \mathcal{N}(0, \sigma^2\Sigma) \\ \epsilon &\sim \mathcal{N}(0, \sigma^2 I),\ \epsilon \perp \mathcal{B} \\ (\tilde{\mathcal{Y}}|\mathcal{B} = b) &\sim \mathcal{N}(X\beta + Zb, \sigma^2 I) \end{aligned}$$

where $\mathcal{N}(\mu, \Sigma)$ denotes the multivariate Gaussian distribution with mean vector μ and variance-covariance matrix Σ, and $\perp$ indicates that two variables are independent. To estimate the coefficient vectors $\beta \in \mathbb{R}^p$, $b \in \mathbb{R}^q$, and the variance parameter σ and sparse (block-diagonal) relative variance-covariance matrix $\Sigma \in \mathbb{R}^{q \times q}$, we use the lme4 package in R written by Douglas Bates and Martin Maechler, which first finds a linear change of coordinates that "spheres" the random effects and then finds the maximum likelihood estimates for β, b, σ, and Σ using penalized iteratively reweighted least-squares, exploiting the sparsity of the random effects matrix to speed computation. For more details see the documentation accompanying the package in the lme4 repository at `http://www.r-project.org/`.

To solve for the maximum likelihood estimates, the design matrix X in equation 2 must be of full column rank. It is well known that this is not the case for a full factorial design matrix with an intercept (as in equation 1), and thus linear combinations ("contrasts") must be used to define the columns of X in order for the fixed-effect coefficients to be estimable. As our designs are balanced (or nearly balanced), we used orthogonal (or nearly orthogonal) Helmert contrasts between the coefficients associated with light on as compared to light off conditions, terminal stimulation as compared to control conditions, and so on, as reported in the main text. Such contrasts allowed us to compare pooled data (e.g., from several sequential light on vs. light off conditions) against each other within a repeated-measures design—yielding improved parameter estimation and test power while accounting for within-animal correlations.

References

1. Aravanis, A.M., *et al.* An optical neural interface: in vivo control of rodent motor cortex with integrated fiberoptic and optogenetic technology. *J Neural Eng* **4**, S143-156 (2007).
2. Gradinaru, V., *et al.* Targeting and readout strategies for fast optical neural control in vitro and in vivo. *J Neurosci* **27**, 14231-14238 (2007).
3. Paxinos, G.a.W., K. *The Mouse Brain in Stereotaxic Coordinates* (Academic Press, 2001).
4. McDonald, A.J., Muller, J.F. & Mascagni, F. GABAergic innervation of alpha type II calcium/calmodulin-dependent protein kinase immunoreactive pyramidal neurons in the rat basolateral amygdala. *J Comp Neurol* **446**, 199-218 (2002).
5. Efron, B. and Tibshirani R. *An Introduction to the Bootstrap* (Chapman and Hall/CRC, 1993).
6. Team, R.D.C. R: A language and environment for statistical computing. (R Foundation for Statistical Computing, Vienna, Austria, 2009).